SUPPLEMENTARY MATERIAL

for

Sortase Independent and Dependent Systems for Acquisition of Haem and Haemoglobin in *Listeria monocytogenes*

Qiaobin Xiao[¤§], Xiaoxu Jiang[¤¶§], Kyle J. Moore[¤], Yi Shao[¤], Hualiang Pi[¤], Iharilalao Dubail[£¥], Alain Charbit[£¥], Salete M. Newton[¤¶] and Phillip E. Klebba[¤¶‡]

[§] Equally contributed to this work

[‡] Address correspondence to peklebba@ou.edu

Tel: 405-325-4969; Fax: 405-325-6111

Supplemental Figure Legends

Figure S1. Synthesis and purification of [59Fe]-Hn. (A) TLC analysis. Synthesis of [^{59}Fe]-Hn using thioglycolic acid was analyzed by thin-layer chromatography (Experimental Procedures); PPIX: protoporphyrin IX; lane 1, standard Hn (Sigma-Aldrich); lane 2, [^{59}Fe]-Hn; lane 3, auto radiograph of lane 2. **(B) UV-visible spectroscopic analysis.** Standard Hn (line 1) and synthesized [^{59}Fe]-Hn were dissolved in 0.1 M NaOH and the absorbances of the freshly made solutions were measured in a Beckman DU-640 spectrophotometer. **(C) ESI mass spectrometry.** Standard Hn (Panel 1) and non-radioactive Hn (panel 2) synthesized by the same protocol as used for [^{59}Fe]-Hn were subjected to mass analysis. Both samples were dissolved in 40% DMSO. In both graphs, two major molecular ion peaks were identified: $(Hn + H)^+$, m/z=616.19, and $(Hn + DMSO + H)^+$, m/z=694.20.

Figure S2. Expression of *L. monocytogenes* binding proteins in *E. coli*, and purification on Ni^{++}-NTA agarose. A. Purification of 6H-FhuD. We cloned the listerial ferric hydroxamate binding protein *fhuD* into pET28a, deleted its signal sequence, and transformed the plasmid into *E. coli* BL21 (Experimental Procedures). The removal of the signal sequence improved its expression in *E. coli* and resulted in cytoplasmic localization. Lanes 2 and 3 contain cytoplasmic extracts of cells carrying the original clone (p6H-FhuD), and lanes 4-7 show cytoplasmic extracts from its derivative p6HΔssFhuD. Lanes 5-7 were obtained from 3 independent transformants of p6HΔssFhuD in BL21. The bacteria from lanes 2 and 4 were not exposed to IPTG; those in lanes 3 and 5-7 were grown with 0.05 mM IPTG for 3 hours prior to harvest. Lanes 8-16 show the elution of 6HΔssFhuD from Ni^{++}-NTA agarose: lanes 8-10, elution by 10 mM imidazole, pH 7.5; lanes 11-16, elution by 50 mM imidazole, pH 7.5. **B. Purification of FhuD, HupD, and 6H-Hbp2.** Homogeneous fractions of 6HΔssFhuD and 6HΔssHupD (lanes 2 and 8, respectively) were incubated with thrombin at 0.04, 0.02, 0.01, and 0.005 Units/uL (lane 3-6 and 9-12, respectively) for 4 h at RT and subjected to SDS-PAGE. The gels were stained with Coomassie Blue R. 6H-Hbp2 was initially extracted from cell lysates by chromatography on the Co^{++}-NTA resin Talon Superflow (Pierce), and peak fractions were further purified on Sephacryl S-100 HR. Lanes 14-18 show the peak fractions from the size exclusion column; 17 and 18 were used in [59Fe]-Hn binding determinations.

Fig. S3. Kinetics of intracellular multiplication in bone-marrow-derived macrophages from BALB/c mice. The figure depicts intracellular survival of the single deletion mutants **(A)** and the triple deletion mutant **(B).** Invasion and intracellular multiplication of the hup deletion mutants was monitored over a 6 h period and compared to that of wild-type EGD-e. Data shown represent the means ± SD of one of at least two independent experiments performed in triplicate with similar results.

Fig. S4. Sortase-independent and dependent pathways of Hn uptake through the Gram-positive cell envelope. A. A schematic representation of the Gram-positive cell wall, assembled from the crystallographic coordinates of its constituents, shows sortase-anchored proteins in the PG matrix and underlying transporters in the phospholipid bilayer of the CM. In several cases, currently unsolved proteins are represented by structurally or functionally related, solved molecules: Hb (PDB file 3HF4), IsdA (2ITF), IsdH (2E7D), SrtA (1T2W), SrtB (1NG5), InlA (1O6V), LmoHbp1 (modeled from IsdC; 2O6P), LmoHbp2 (from IsdC; 2O6P), LmoFhuDGBC (from EcoMalEFGK; 3FH6), LmoHupDGC (from Hin Fe-ABC transporter; 2NQ2). The putative ABC transporter of the *L.monocytogenes srtB* operon, encoded by *lmo2182-4*, was modeled from EcoBtuCDF (2QI9). PG, shown in wire format (coordinates were kindly provided by S. Mobashery), was assembled as polymers with 16-residue glycan backbones in the vertical scaffold model, according to Meroeuh et al. (2006). In the sortase-dependent pathway of Hn uptake, the PG matrix may constitute a barrier to Hb diffusion, from which sortase-anchored proteins (listerial Hbp and/or staphylococcal Isd proteins) scavenge iron and pass the porphyrin among binding proteins that ultimately transfer it to ABC transporters like HupDGC and FhuDGBC in the CM . **B.** The image in panel A was rotated on a horizontal axis to view the honeycomb PG matrix, rendered in a space-filling, molecular-surface format and colored brown, from the cell exterior. This view shows the sortase-independent pathway of Hn uptake: the large pores (20-50 Å; Demchick & Koch, 1996; Touhami et al., 2004; Meroueh et al., 2006) of the PG polymer allow permeation of small molecules like ferric siderophores and Hn, which lipoprotein binding proteins of ABC transporters in the CM adsorb for uptake.

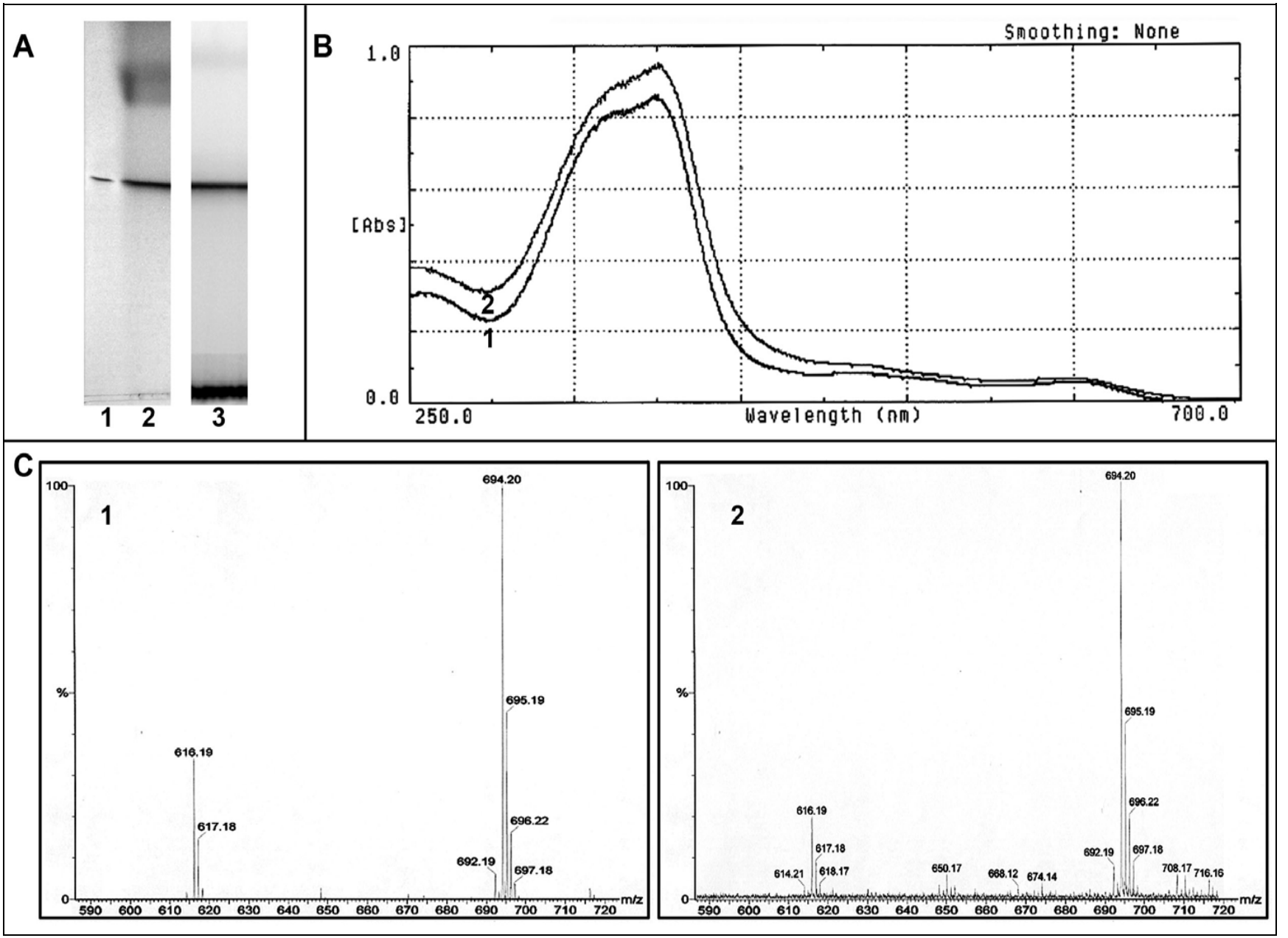
A
1 2 3
B
Smoothing: None
1.0
[Abs]
0.0
2
1
250.0
Wavelength (nm)
700.0
C
1
100
%
0
694.20
695.19
616.19
696.22
617.18
692.19
697.18
590 600 610 620 630 640 650 660 670 680 690 700 710 720
m/z
2
100
%
0
694.20
695.19
696.22
616.19
617.18
692.19
697.18
614.21
618.17
650.17
668.12
674.14
708.17
716.16
590 600 610 620 630 640 650 660 670 680 690 700 710 720
m/z

Figure S1

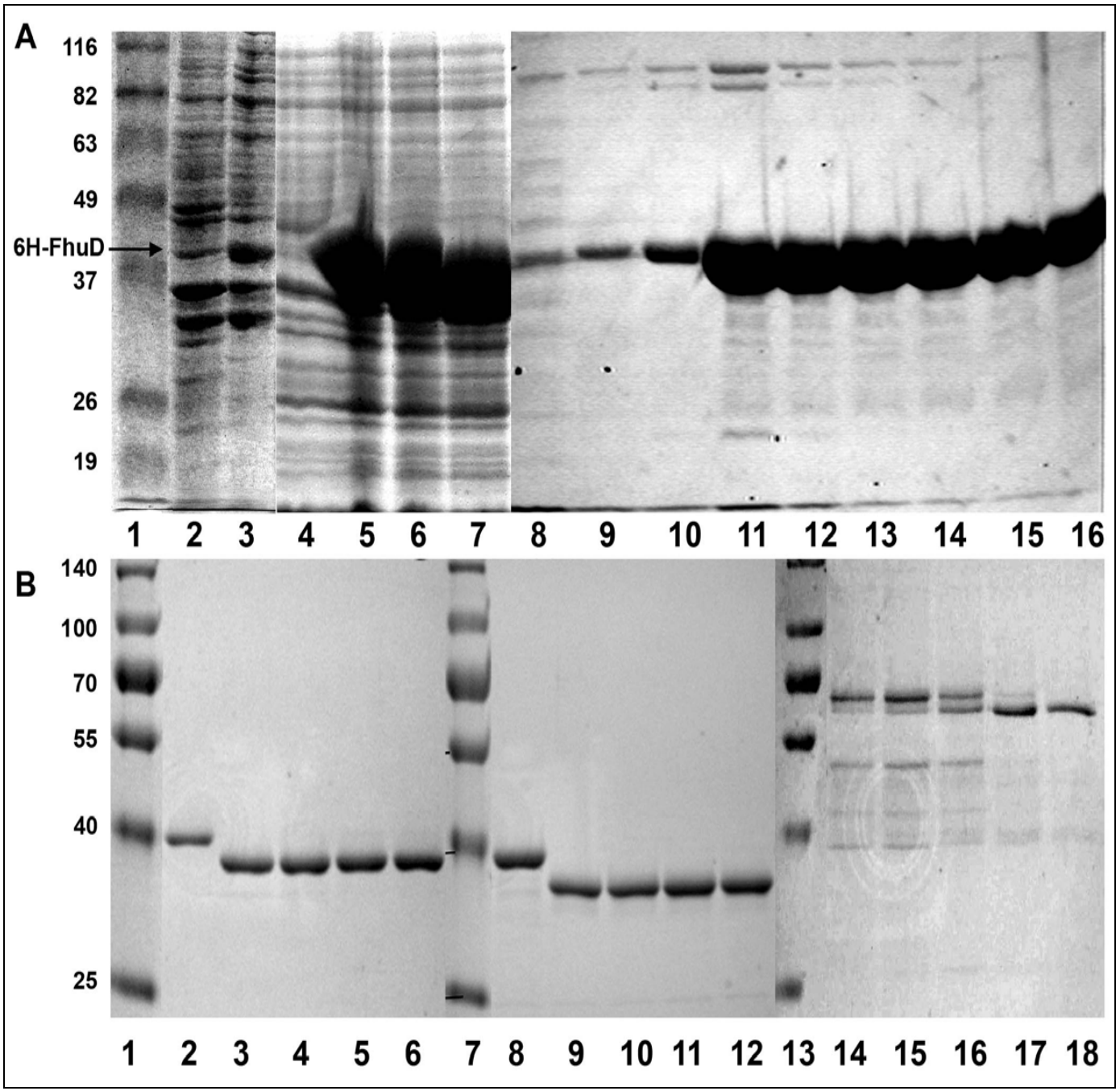
A
116
82
63
49
6H-FhuD
37
26
19
1 2 3 4 5 6 7 8 9 10 11 12 13 14 15 16
B
140
100
70
55
40
25
1 2 3 4 5 6 7 8 9 10 11 12 13 14 15 16 17 18

Figure S2

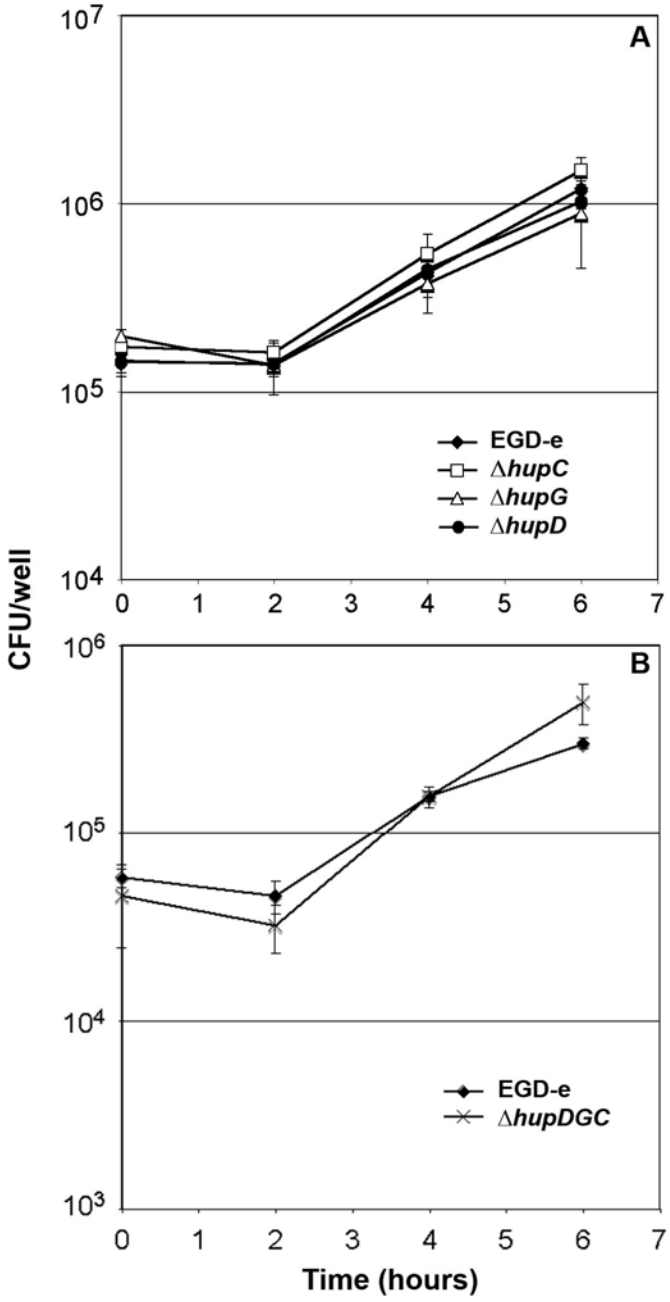

Figure S3.

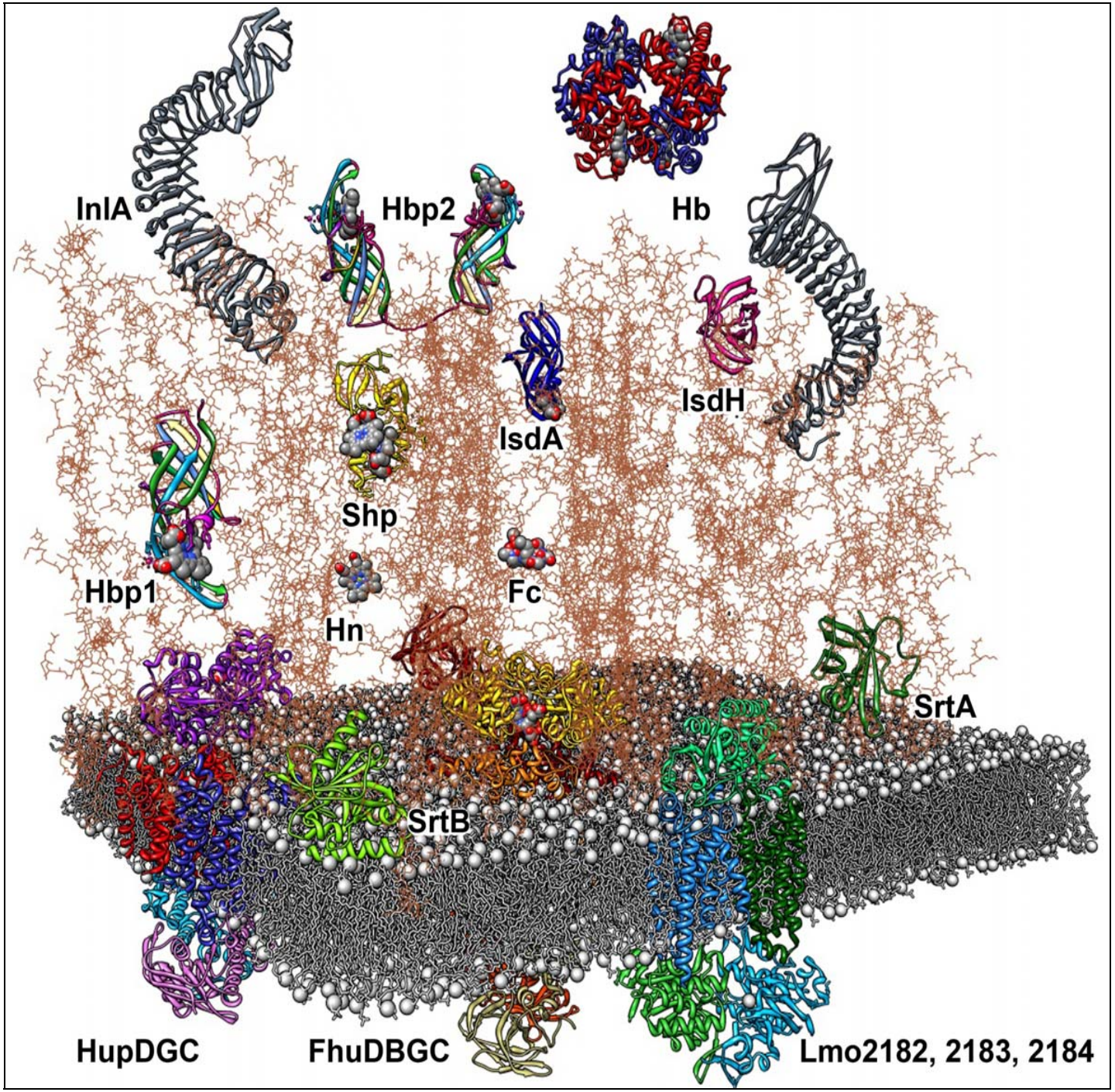
InlA
Hbp2
Hb
IsdH
IsdA
Shp
Fc
Hbp1
Hn
SrtA
SrtB
HupDGC
FhuDBGC
Lmo2182, 2183, 2184

Fig S4a

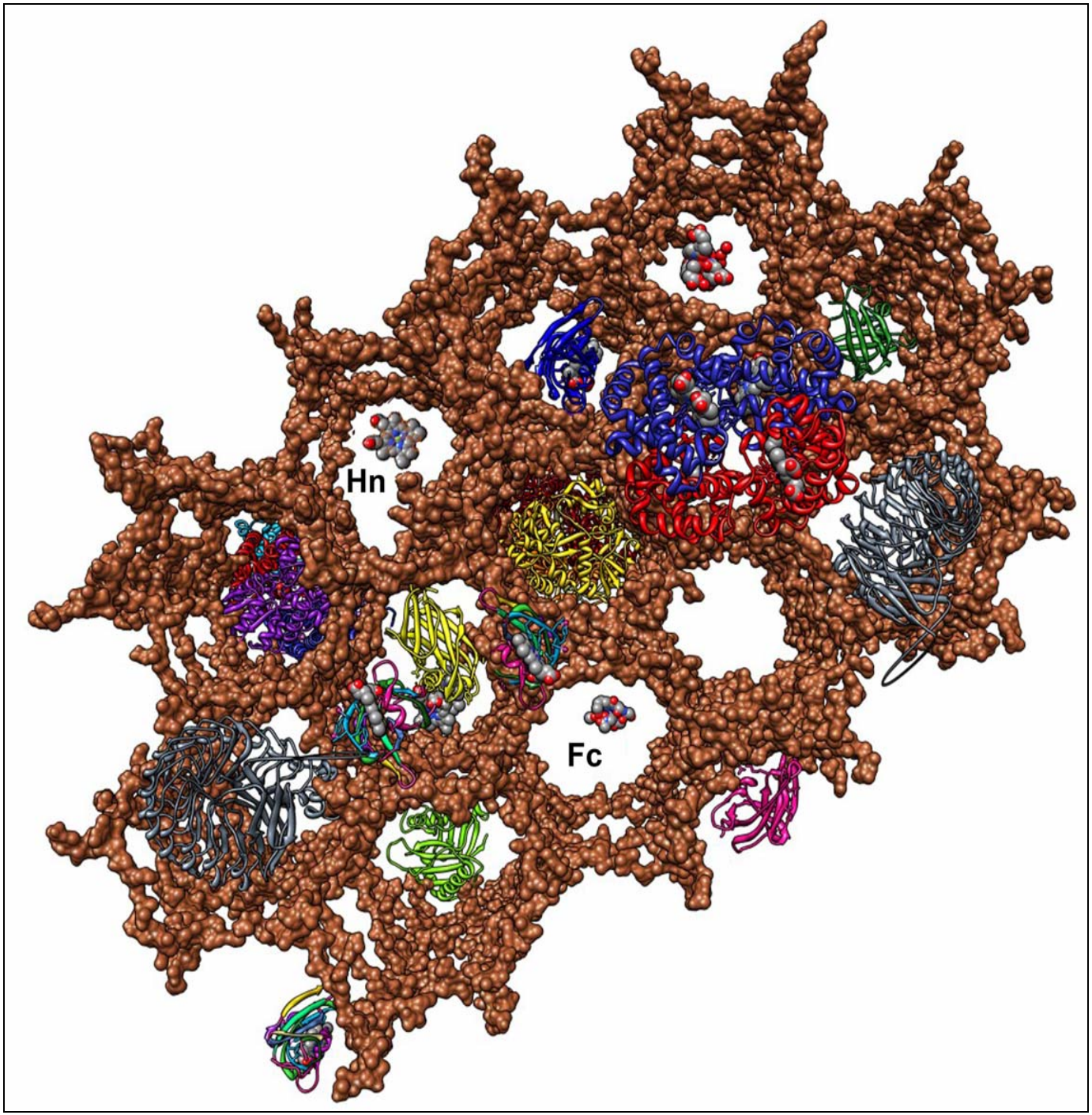

Fig S4b